The first example of a significant active site conformational rearrangement in a carbonic anhydrase-inhibitor adduct: the carbonic anhydrase I–topiramate complex

Vincenzo Alterio,[a] Simona Maria Monti,[a] Emanuela Truppo,[a] Carlo Pedone,[a] Claudiu T. Supuran*[b] and Giuseppina De Simone*[a]

Received 23rd December 2009, Accepted 28th April 2010
First published as an Advance Article on the web 27th May 2010
DOI: 10.1039/b926832d

Topiramate is a widely used antiepileptic drug, which has been demonstrated to act as an efficient weight loss agent. Since several studies have pointed out that **TPM** is a potent *in vitro* inhibitor of several Carbonic anhydrase (CA) isozymes, it has been hypothesized that its anti-obesity properties could be ascribed to the inhibition of the CAs involved in *de novo* lipogenesis. Consequently, the study of the interactions of **TPM** with all human CA isoforms represents an important step for the rational drug design of selective CA inhibitors to be used as anti-obesity drugs. In this paper we report the crystallographic structure of the adduct that **TPM** forms with hCA I, showing for the first time a profound reorganization of the CA active site upon binding of the inhibitor. Moreover, a structural comparison with hCA II–**TPM** and hCA VA–**TPM** adducts, previously investigated, has been performed showing that a different H-bond network together with the movement of some amino acid residues in the active site may account for the different inhibition constants of **TPM** toward these three CA isozymes.

Introduction

A wealth of X-ray structural data have been accumulated in the last 15 years for carbonic anhydrase (CA, EC 4.2.1.1)–inhibitor complexes, including the three main classes of inhibitors: (i) the pharmacologically relevant sulfonamides and their isosteres (sulfamates, sulfamides, ureates and hydroxamates); (ii) the simple inorganic anions and (iii) the coumarins.[1,2] However, although X-ray crystal structures are already available for the majority of the twelve catalytically active members of the human CA family (*i.e.*, isozymes I-VA, IX, XII, XIII and XIV),[3–12] most of the reported complexes with inhibitors involve just isozyme II (and to a lesser extent isozyme I). These data are tremendously important for the drug design of isozyme-selective CA inhibitors (CAIs), a goal largely unattained for the moment but for which important advances have been made in the last years. Indeed, CAIs have applications as diuretics, antiglaucoma, antiobesity and antitumor agents/diagnostic tools, and they target different CA isozymes of the 16 presently known from vertebrates.[13]

The CA active site (of all α-CA isozymes crystallized so far) possesses two distinctive features: (*i*) a well defined separation into two regions, one lined with hydrophobic and the other with hydrophilic amino acid residues, leading to a highly distinct active site architecture, which strongly influences the binding of substrates, inhibitors and activators;[1] (*ii*) a rigid 3D structure of the protein backbone. Indeed, no modification of the protein backbone has been reported when inhibitors, activators and substrates bind to the enzyme cavity.[1] Moreover, except His64, which acts as a proton shuttle in the catalytic cycle and which has a flexible side chain, and Phe131 in two CA II/inhibitor complexes,[14,15] the side chain conformation of residues delimiting the active site cavity is highly maintained after ligand binding. It should be mentioned that this distinctive feature of the CA active site architecture is little understood at the present time.

Among the various applications of CAIs, obesity has only recently started to be considered, with the mitochondrial isoforms CA VA and VB being the possible targets for such drugs.[16–19] Indeed, obesity is a growing widespread medical problem, which has been recognized as a critical global health issue, since it presently encroaches on over 300 million individuals worldwide.[19–26]

Topiramate[27–32] (**TPM**) (Fig. 1) is a sulfamate-substituted monosaccharide, marketed worldwide for the treatment of epilepsy[33] and prophylaxis of migraine.[34]

TPM anticonvulsant effects are due to a complex mechanism of action which involves (*i*) blockage of voltage-activated sodium channels, (*ii*) enhancement of the activity of the neurotransmitter gamma-aminobutyrate (GABA) at some subtypes of the GABAA receptors, and (*iii*) antagonism of the ability of kainate to activate the kainate/AMPA (non-NMDA) subtype of glutamate receptors.[27–32] Recently, **TPM** is being used in a growing number of other applications[35] such as treatment of bipolar disorder[36] and post traumatic stress disorder,[37] and investigated for use in treating several other pathologies such as bulimia nervosa,[38] obsessive-compulsive disorder,[39] idiopathic intracranial hypertension,[40] neuropathic pain[41] and infantile spasms.[42] Obesity is among the pathologies that have been recently explored for treatment with **TPM**.[43] Indeed data from studies of **TPM** performed on several

[a]*Istituto di Biostrutture e Bioimmagini-CNR, via Mezzocannone 16, 80134 Naples, Italy. E-mail: gdesimon@unina.it; Fax: +39-081-2536642; Tel: +39-081-2534579*
[b]*Università degli Studi di Firenze, Laboratorio di Chimica Bioinorganica, Rm. 188, Via della Lastruccia 3, I-50019 Sesto Fiorentino (Firenze), Italy. E-mail: claudiu.supuran@unifi.it; Fax: +39-055-4573385; Tel: +39-055-4573005*

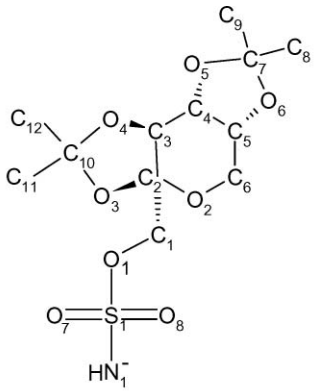

(K_I for CA I= 250 nM; K_I for CA II= 10 nM; K_I for CA VA= 63 nM)

Fig. 1 **TPM** chemical structure, crystallographic numbering, and its inhibitory activity against hCA I, II and VA.

animal models have demonstrated the efficacy of this drug as a weight loss agent[44] and have led to clinical trials of **TPM** for treatment of obesity.[43] Some authors suggested that the anti-obesity action of **TPM** could be ascribed to its anti-glutamatergic properties, but no precise data supporting this hypothesis are available yet.[45] However, our group[46] demonstrated that **TPM** is a potent *in vitro* inhibitor of several CA isozymes (see Fig. 1), suggesting that the anti-obesity effects of this drug could be ascribed to the inhibition of CAs involved in *de novo* lipogenesis, namely CA VA or/and CA VB within the mitochondria as well as CA II within the cytosol.[16–19,47] In agreement with this hypothesis, several other studies have provided evidence that CAIs have potential as anti-obesity drugs.[13] The crystal structure[46,48] and a molecular modeling study[49] of the adducts that **TPM** forms with hCA II and hCA VA have also been published, showing the molecular basis responsible for the high affinity of **TPM** for the active sites of these CA isozymes. Altogether these findings suggested that the use of **TPM** as a lead molecule for the design of CA inhibitors targeting isozymes involved in lipogenesis could represent a possible new approach for the treatment and prophylaxis of obesity. In this context the study of the interactions of **TPM** with all human CA isoforms represents an important step for the rational drug design of selective CA VA/VB inhibitors to be used as anti-obesity drugs. In this paper we report the crystallographic structure of the adduct that **TPM** forms with hCA I, showing for the first time that a massive reorganization deep within the active site is necessary in order to allow inhibitor binding. Moreover, a structural comparison with hCA II–**TPM** and hCA VA–**TPM** adducts has been performed, providing a reasonable explanation of the different affinities which this drug shows toward these three isoforms.

Results and discussion

The hCA I–**TPM** complex was crystallized in the space group $P2_12_12_1$, with two molecules per asymmetric unit (called **A** and **B**). The structure was solved by molecular replacement using native hCA I[3] as the starting model and refined with the CNS program to a crystallographic R_{factor} of 19.9% and an R_{free} of 22.8% in the 20.00–1.90 Å resolution range (Table 1).

Table 1 Data collection and refinement statistics. Values in parentheses refer to the highest resolution shell (1.97–1.90 Å)

Crystal parameters	
Space group	$P2_12_12_1$
a/Å	63.32
b/Å	71.07
c/Å	120.66
Independent molecules	2
Data collection statistics	
Resolution/Å	20.00–1.90
Wavelength/Å	1.0
T/K	100
R_{merge} (%)[a]	6.7 (33.4)
Mean I/σ(I)	21.2 (2.3)
Total reflections	220776
Unique reflections	41817
Completeness (%)	95.7 (74.5)
Refinement	
Resolution/Å	20.00–1.90
R_{factor} (%)[b]	19.9
R_{free} (%)[b]	22.8
RMSD from ideal geometry:	
Bond lengths/Å	0.007
Bond angles (°)	1.4
Number of protein atoms	4016
Number of inhibitor atoms	44
Number of water molecules	470
Average B factor/Å^2:	
All atoms	27.0
Protein atoms	25.9
Water molecules	36.2

[a] $R_{merge} = \Sigma\,|I_i - < I >|\,/\Sigma I_i$; over all reflections. [b] $R_{factor} = \Sigma\,||F_o| - |F_c||\,/\Sigma |F_o|$; R_{free} calculated with 5% of data withheld from refinement.

The two independent molecules in the asymmetric unit overlapped quite well; indeed, the superimposition carried out on the backbone positions of all 256 residues led to an RMSD of 0.2 Å. Furthermore, all residues delimiting the active site region adopted an identical conformation within the two molecules. Consequently, the following discussion will be conducted based on only one arbitrarily chosen molecule, unless otherwise stated. A clear electron density for the **TPM** molecule was evident within each molecule in the asymmetric unit (Fig. 2).

The main interactions of the inhibitor with protein are shown in Fig. 3A. The ionized sulfamate NH^- group of **TPM** is coordinated to the Zn^{2+} ion ($Zn^{2+}\cdots$**TPM**N1 = 2.00 Å), and donates a hydrogen bond to Thr199OG1 (Thr199OG1$\cdots$**TPM**N1 = 2.71 Å), while one of the two sulfamate oxygens accepts a hydrogen bond from the backbone amide group of the same residue (Thr199N$\cdots$**TPM**O7 = 2.90 Å). Several other polar interactions are observable between the sugar moiety of the inhibitor and the enzyme active site. In particular, **TPM**O6 and **TPM**O4 atoms of the inhibitor are hydrogen bonded to His64NE2 (His64NE2$\cdots$**TPM**O6 = 3.04 Å) and Gln92NE2 (Gln92NE2$\cdots$**TPM**O4 = 3.46 Å), respectively (Fig. 3A), while **TPM**O2 and **TPM**O3 atoms are engaged in a bifurcated hydrogen bond with a water molecule (**TPM**O2$\cdots$HOH442 = 2.88 Å; **TPM**O3$\cdots$HOH442 = 3.03 Å), which in turn interacts with

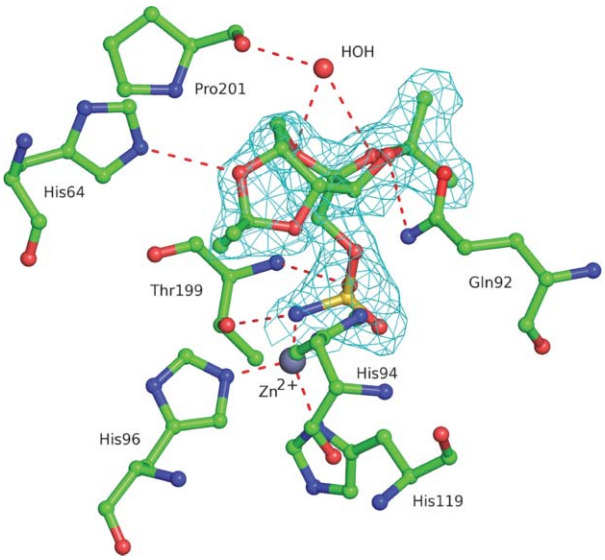

Fig. 2 Active site region of the hCAI–**TPM** complex. The simulated annealing omit map, calculated with Fourier coefficients $|2F_o–F_c|$, relative to the inhibitor molecule is shown. Zn^{2+} coordination and hydrogen bonds are also shown as dotted lines.

the carboxyl group of Pro201 (Pro201O $\cdots$ HOH442 = 2.83 Å). Several other strong van der Waals interactions (distance <4.5 Å) (Fig. 3A) contribute to the stabilization of the complex.

A comparison of the hCA I structure in the complex under investigation with the native enzyme shows that a significant conformational rearrangement is necessary in the active site in order to allow the binding of the inhibitor (Fig. 4A).

This fact has never before been evidenced in CA–inhibitor adducts, as the active site of this protein is a highly rigid one.[1] Indeed, due to the fact that in hCA I the residue in position 200 is a bulky one (His) whereas in all other isoforms it is a threonine or a valine, the bulky sugar moiety of the **TPM** molecule cannot enter the enzyme active site without the displacement of Trp5, His67 and His200 residues. The latter residue in the native structure forms a hydrogen bond with Pro201 (His200ND1 $\cdots$ Pro201O = 2.82 Å), which is lost in the complex with consequent formation of a new hydrogen bond with Tyr7 (His200ND1 $\cdots$ Tyr7OH = 2.95 Å). Since all these residues present a well conserved conformation within various CA–inhibitor complexes,[1,50–57] it is reasonable to hypothesize that their movement requires a considerable energy cost. This finding is in agreement with the observation that, despite the presence of a large number of polar and hydrophobic interactions between the enzyme and the inhibitor, this latter does not show high affinity toward the enzyme with an inhibition constant of only 250 nM. It is important to highlight that this is the first evidence of such a large active site rearrangement in a CA–inhibitor complex, which we consider an important finding of the present study.

A detailed comparative analysis of the **TPM** inhibition constants for various CAs (see Fig. 1) revealed that **TPM** binds human isozyme I with an efficiency significantly lower than that measured for hCA II and hCA VA (*i.e.*, around 25 times less for hCA II and around 4 times less for hCA VA). To identify the molecular features that could be responsible for such behavior, a detailed structural comparison between the adducts that **TPM** forms with these three isoforms[46,48,49] has been performed. hCA I, hCA II and hCA VA share a high degree of sequence homology and several residues that in hCA I are involved in **TPM** recognition are also conserved in hCA II and hCA VA (Fig. 5).

Consequently the interaction of the **TPM** molecule within the three active sites is rather similar. However, amino acid substitutions at positions 62 and 200 determine important differences in inhibitor binding. The main protein–inhibitor interactions observed in the hCA II–**TPM** and hCA VA–**TPM** structures are schematically depicted in Fig. 3B and 3C, respectively. In both cases, as observed for hCA I–**TPM** and other CA–sulfamate complexes,[1] the **TPM** sulfamate moiety is tetrahedrally coordinated to the zinc ion of the enzyme *via* its deprotonated nitrogen atom and hydrogen bonded to the Thr199 residue. An extended network of polar interactions between the sugar scaffold of the inhibitor and protein residues Asn62, Gln92 and Thr200 in the case of hCA II, and Gln92 and Thr200 in the case of hCA VA is observed (see Fig. 3B and 3C). The presence of an additional H-bond interaction in the case of the hCA II–**TPM** complex could be responsible for the higher affinity of **TPM** toward hCA II (K_i value = 10 nM) with respect to hCA VA (K_i value = 63 nM) but does not explain such a big difference with hCA I. However, the comparison of the hCA II structure in complex with **TPM** with that of native enzyme reveals that the binding of **TPM** to hCA II does not cause any significant movement of the active site residues (see fig. 4B), which is different from what is observed for hCA I. This different behavior can explain the difference in the

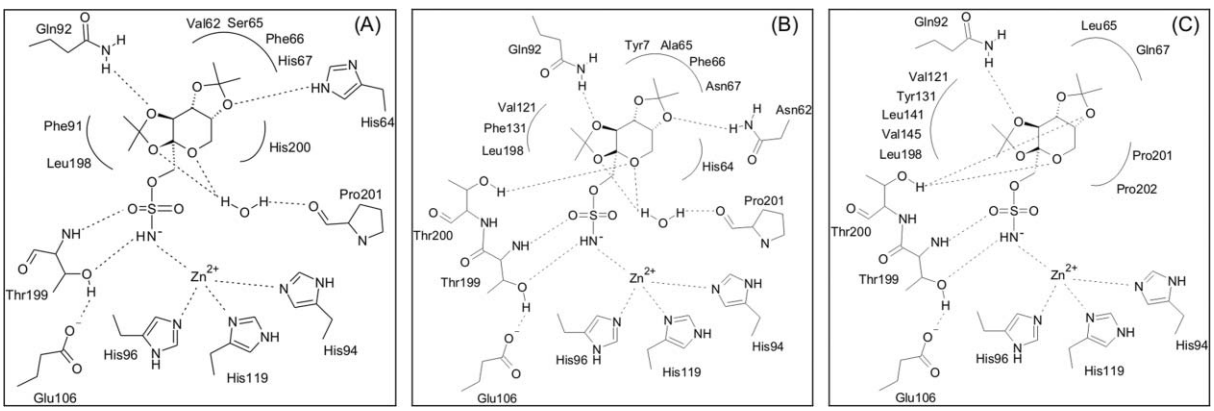

Fig. 3 Schematic representation of **TPM** binding within the hCA I (A), hCA II (B)[46,48] and hCA (VA)[49] active sites.

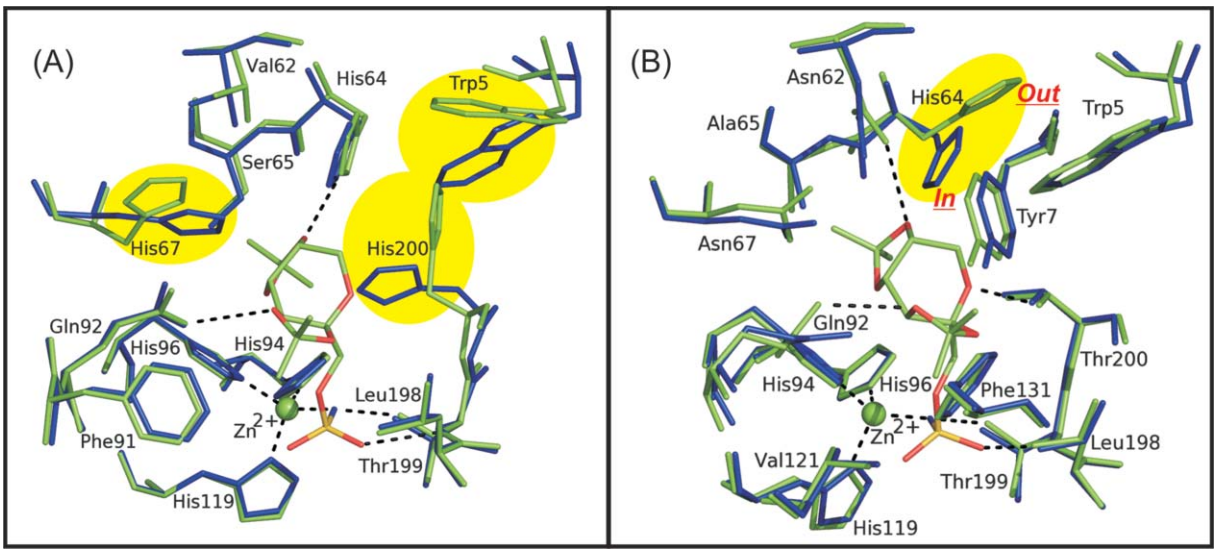

Fig. 4 (A) Superposition of the 3D structures of hCA I in the native state (blue) (PDB code 2CAB)[3] with hCA I in complex with **TPM** (green). (B) Superposition of the structures of hCA II in the native state (blue) (PDB code 1CA2)[4] with hCA II in complex with **TPM** (green) (PDB code 3HKU).[46,48]

```
hCA I     1  ASPDWGYDDKNGPEQWSKLYPIANGNNQSPVDIKTSETKHDTSLKPISVSYNPATAKEIINVGHSFHV
hCA II    2  -SHHWGYGKHNGPEHWHKDFPIAKGERQSPVDIDTHTAKYDPSLKPLSVSYDQATSLRILNNGHAFNV
hCA VA    3  --CAWQTSNNTLHPLWTVPVSVPGGTRQSPINIQWRDSVYDPQLKPLRVSYEAASCLYIWNTGYLFQV

hCA I    69  NFEDNDNRSVLKGGPFSDSYRLFQFHFHWGSTNEHGSEHTVDGVKYSAELHVAHWNSAKYSSLAEAAS
hCA II   69  EFDDSQDKAVLKGGPLDGTYRLIQFHFHWGSLDGQGSEHTVDKKKYAAELHLVHWNT-KYGDFGKAVQ
hCA VA   69  EFDDATEASGISGGPLENHYRLKQFHFHWGAVNEGGSEHTVDGHAYPAELHLVHWNSVKYQNYKEAVV
                                  * *     *       *
hCA I   137  KADGLAVIGVLMKVGEANPKLQKVLDALQAIKTKGKRAPFTNFDPSTLLPSSLDFWTYPGSLTHPPLY
hCA II  137  QPDGLAVLGIFLKVGSAKPGLQKVVDVLDSIKTKGKSADFTNFDPRGLLPESLDYWTYPGSLTTPPLL
hCA VA  137  GENGLAVIGVFLKLGAHHQTLQRLVDILPEIKHKDARAAMRPFDPSTLLPTCWDYWTYAGSLTTPPLT
                                                                        *

hCA I   205  ESVTWIICKESISVSSEQLAQFRSLLSNVEGDNAVPMQHNNRPTQPLKGRTVRASF---------
hCA II  205  ECVTWIVLKEPISVSSEQVLKFRKLNFNGEGEPEELMVDNWRPAQPLKNRQIKASFK--------
hCA VA  205  ESVTWIIQKEPVEVAPSQLSAFRTLLFSALGEEEKMMVNNYRPLQPLMNRKVWASFQATNEGTRS
```

Fig. 5 Sequence alignment of hCA I, hCA II and hCA VA. Strictly conserved residues are highlighted in gray, catalytic histidines, Thr199 and Glu106 are starred, while residues delimiting the active site cavity are boxed.

affinity of **TPM** toward hCA II and hCA I and further confirms the role of the movement of the active site residues in determining the enzyme–inhibitor affinity. Since no native structure is available in the case of hCA VA it is not possible to clarify if in this case a movement of the active site residues is present or not.

Conclusions

In conclusion, the X-ray structure of hCA I–**TPM** adduct here reported, together with the comparison with the hCA II–**TPM** and hCA VA–**TPM** complex structures previously investigated, suggest that a different H-bond network together with the movement of some amino acid residues in order to accommodate the inhibitor, may account for the different inhibition constants of **TPM** toward these three CA isozymes. These data may be helpful in the design of CAIs selective for various isozymes (*e.g.*, CA VA/VB, etc) with potential as anti-obesity drugs or other pharmaceutical applications. It should also be mentioned that hCA I itself may be a drug target for designing agents for the treatment of diabetic retinopathy,[58,59] although this field has been scarcely investigated to date. The evidence presented here regarding the profound reorganization of the hCA I active site upon binding of the inhibitor is also the first such example in the literature and might be useful for designing CAIs which exploit it.

Experimental

Crystallization and X-ray data collection

hCA I was purchased by Sigma and further purified on NHS-activated Sepharose 4 FF resin (GE Healthcare) preactivated with pAMBS (Sigma) as previously reported.[11] Eluted protein was concentrated to 10 mg ml^{-1} and used for crystallization experiments. The hCA I–**TPM** complex was obtained by adding a 5-molar excess of the inhibitor to a 10 mg mL^{-1} protein solution in 50 mM TRIS-SO_4, pH 8.5. Crystals of the complex were obtained by the hanging drop vapor diffusion technique at 20 °C. Drops were prepared by mixing 1 μL of the hCA I–**TPM** adduct with 1 μL of precipitant solution (30% (w/v) polyethylene glycol 4000, 0.2 M sodium acetate, 0.1 M TRIS-HCl, pH 8.5), and equilibrated over a well containing 1 mL of precipitant solution. Crystals appeared in the drops after two days and grew in about one week to maximum dimensions of 0.2 × 0.3 × 0.3 mm^3. X-ray diffraction data were

collected at 100 K, at the Synchrotron source Elettra in Trieste, Italy, using a Mar CCD detector. Prior to cryogenic freezing, the crystals were transferred to the precipitant solution with the addition of 15% (v/v) glycerol. The data were processed using the HKL2000 package.[60] The crystals belonged to the space group $P2_12_12_1$ with unit cell dimension of $a = 63.32$ Å, $b = 71.07$ Å, and $c = 120.66$ Å. The Matthews coefficient ($V_M = 2.4$ Å^3/Da) indicated that the crystallographic asymmetric unit contained two molecules according to a solvent content of 48%. Data collection statistics are reported in Table 1.

Structure determination and refinement

The structure of the hCA I–**TPM** complex was solved by molecular replacement technique using the program AMoRe[61] and the crystallographic coordinates of the native hCA I (PDB code 2CAB)[3] as model template. Refinement of the structure was carried out using CNS[62] and model building was performed with O.[63] Clear electron density for one inhibitor molecule in each active site was observed in the $|F_o| - |F_c|$ maps. Inhibitor molecules were gradually built into the model over several rounds of refinement. Restraints on inhibitor bond angles and distances were taken from similar structures in the Cambridge Structural Database and standard restraints were used on protein bond angles and distances throughout refinement. The correctness of stereochemistry was finally checked using PROCHECK.[64] Refinement statistics are summarized in Table 1.

Coordinates and structure factors have been deposited in the Protein Data Bank (accession code 3LXE).

Abbreviations

AMPA	(α-amino-3-hydroxy-5-methyl-4-isoxazolepropionic acid)
CAI	(carbonic anhydrase inhibitor)
GABA	(γ-aminobutyric acid)
hCA	(human carbonic anhydrase)
NMDA	(*N*-methyl-D-aspartic acid)
pAMBS	(*p*-aminomethylbenzenesulfonamide)
RMSD	(root mean square deviation)
TPM	(topiramate)
TRIS-HCl	(2-amino-2-(hydroxymethyl)-1,3-propanediol, hydrochloride)

Acknowledgements

This work was financed by a EU project of the 6th framework programme (DeZnIT project, contract No. LSHB-CT-2007-037303). We thank the Sincrotrone Trieste C.N.R./Elettra, for giving us the opportunity to collect data at the Crystallographic Beamline.

References

1 V. Alterio, A. Di Fiore, K. D'Ambrosio, C. T. Supuran and G. De Simone, in *Drug Design of Zinc-Enzyme Inhibitors: Functional, Structural, and Disease Applications*, Eds C. T. Supuran and J. Y. Winum, Wiley, Hoboken, 2009, pp. 73–138.
2 A. Maresca, C. Temperini, H. Vu, N. B. Pham, S. A. Poulsen, A. Scozzafava, R. J. Quinn and C. T. Supuran, *J. Am. Chem. Soc.*, 2009, **131**, 3057–3062.
3 K. K. Kannan, M. Ramanadham and T. A. Jones, *Ann. N. Y. Acad. Sci.*, 1984, **429**, 49–60.
4 A. E. Eriksson, T. A. Jones and A. Liljas, *Proteins: Struct., Funct., Genet.*, 1988, **4**, 274–282.
5 A. E. Eriksson and A. Liljas, *Proteins: Struct., Funct., Genet.*, 1993, **16**, 29–42.
6 D. M. Duda, C. Tu, S. Z. Fisher, H. An, C. Yoshioka, L. Govindasamy, P. J. Laipis, M. Agbandje-McKenna, D. N. Silverman and R. McKenna, *Biochemistry*, 2005, **44**, 10046–10053.
7 T. Stams, S. K. Nair, T. Okuyama, A. Waheed, W. S. Sly and D. W. Christianson, *Proc. Natl. Acad. Sci. U. S. A.*, 1996, **93**, 13589–13594.
8 P. A. Boriack-Sjodin, R. W. Heck, P. J. Laipis, D. N. Silverman and D. W. Christianson, *Proc. Natl. Acad. Sci. U. S. A.*, 1995, **92**, 10949–10953.
9 V. Alterio, M. Hilvo, A. Di Fiore, C. T. Supuran, P. Pan, S. Parkkila, A. Scaloni, J. Pastorek, S. Pastorekova, C. Pedone, A. Scozzafava, S. M. Monti and G. De Simone, *Proc. Natl. Acad. Sci. U. S. A.*, 2009, **106**, 16233–16238.
10 D. A. Whittington, A. Waheed, B. Ulmasov, G. N. Shah, J. H. Grubb, W. S. Sly and D. W. Christianson, *Proc. Natl. Acad. Sci. U. S. A.*, 2001, **98**, 9545–9550.
11 A. Di Fiore, S. M. Monti, M. Hilvo, S. Parkkila, V. Romano, A. Scaloni, C. Pedone, A. Scozzafava, C. T. Supuran and G. De Simone, *Proteins: Struct., Funct., Bioinf.*, 2008, **74**, 164–175.
12 D. A. Whittington, J. H. Grubb, A. Waheed, G. N. Shah, W. S. Sly and D. W. Christianson, *J. Biol. Chem.*, 2004, **279**, 7223–7228.
13 C. T. Supuran, *Nat. Rev. Drug Discovery*, 2008, **7**, 168–181.
14 A. Di Fiore, C. Pedone, K. D'Ambrosio, A. Scozzafava, G. De Simone and C. T. Supuran, *Bioorg. Med. Chem. Lett.*, 2006, **16**, 437–442.
15 L. W. Woo, D. S. Fischer, C. M. Sharland, M. Trusselle, P. A. Foster, S. K. Chander, A. Di Fiore, C. T. Supuran, G. De Simone, A. Purohit, M. J. Reed and B. V. Potter, *Mol. Cancer Ther.*, 2008, **7**, 2435–2444.
16 C. T. Supuran, A. Di Fiore and G. De Simone, *Expert Opin. Emerging Drugs*, 2008, **13**, 383–392.
17 G. De Simone and C. T. Supuran, in *Drug Design of Zinc-Enzyme Inhibitors: Functional, Structural, and Disease Applications*, eds C. T. Supuran and J. Y. Winum, Wiley, Hoboken, 2009, pp. 241-254.
18 G. De Simone, A. Di Fiore and C. T. Supuran, *Curr. Pharm. Des.*, 2008, **14**, 655–660.
19 G. De Simone and C. T. Supuran, *Curr. Top. Med. Chem.*, 2007, **7**, 879–884.
20 J. C. G. Halford, *Appetite*, 2006, **46**, 6–10.
21 L. A. Campfield, F. J. Smith and P. Burn, *Science*, 1998, **280**, 1383–1387.
22 H. E. Bays, *Obesity*, 2004, **12**, 1197–1211.
23 J. M. Friedman, *Science*, 2003, **299**, 856–859.
24 J. O. Hill, H. R. Wyatt, G. W. Reed and J. C. Peters, *Science*, 2003, **299**, 853–855.
25 L. L. Ioannides-Demos, J. Proietto, A. M. Tonkin and J. J. McNeil, *Drug Saf.*, 2006, **29**, 277–302.
26 R. S. Padwal and S. R. Majumdar, *Lancet*, 2007, **369**, 71–77.
27 R. P. Shank, J. F. Gardocki, J. L. Vaught, C. B. Davis, J. J. Schupsky, R. B. Raffa, S. J. Dodgson, S. O. Nortey and B. E. Maryanoff, *Epilepsia*, 1994, **35**, 450–460.
28 H. L. Edmonds, Y. D. Jiang, P. Y. Zhang and R. P. Shank, *Life Sci.*, 1996, **59**, PL127–131.
29 J. L. Stringer, *Epilepsy Res.*, 2000, **40**, 147–153.
30 A. Sabers and L. Gram, *Drugs*, 2000, **60**, 23–33.
31 B. F. D. Bourgeois, *Journal of Child Neurology*, 2000, **15**, S27–30.
32 M. Bialer, S. I. Johannessen, H. J. Kupferberg, R. H. Levy, P. Loiseau and E. Perucca, *Epilepsy Res.*, 2001, **43**, 11–58.
33 K. A. Lyseng-Williamson and L. P. Yang, *Drugs*, 2007, **67**, 2231–2256.
34 N. M. Ramadan and T. M. Buchanan, *Pharmacol. Ther.*, 2006, **112**, 199–212.
35 N. Mirza, A. G. Marson and M. Pirmohamed, *Br. J. Clin. Pharmacol.*, 2009, **68**, 655–661.
36 K. Vasudev, K. Macritchie, J. Geddes, S. Watson and A. Young, *Cochrane Database of Systematic Reviews*, 2006, (Issue 1). Art. No.: CD003384.
37 H. A. Berlin, *Current Psychiatry Reports*, 2007, **9**, 291–300.
38 S. L. McElroy, A. I. Guerdjikova, B. Martens, P. E. Jr Keck, H. G. Pope and J. I. Hudson, *CNS Drugs*, 2009, **23**, 139–156.
39 E. Hollander and B. Dell'Osso, *International Clinical Psychopharmacology*, 2006, **21**, 189–191.
40 N. Celebisoy, F. Gökçay, H. Sirin and O. Akyürekli, *Acta Neurol. Scand.*, 2007, **116**, 322–327.
41 E. A. Bendaly, C. A. Jordan, S. S. Staehler and D. A. Rushing, *Supportive Cancer Therapy*, 2007, **4**, 241–246.

42 L. P. Zou, Q. Lin, J. Qin, F. C. Cai, Z. S. Liu and E. Mix, *Clinical Neuropharmacology*, 2008, **31**, 86–92.
43 A. Astrup and S. Toubro, *Obesity*, 2004, **12**, 167S–173S.
44 D. Richard, F. Picard, C. Lemieux, J. Lalonde, P. Samson and Y. Deshaies, *Int. J. Obes.*, 2002, **26**, 344–353.
45 M. C. Mancini and A. Halpern, *Expert Opin. Invest. Drugs*, 2006, **15**, 897–915.
46 A. Casini, J. Antel, F. Abbate, A. Scozzafava, S. David, H. Waldeck, S. Schäfer and C. T. Supuran, *Bioorg. Med. Chem. Lett.*, 2003, **13**, 841–845.
47 W. R. Chegwidden and I. M. Spencer, *Comp. Biochem. Physiol.*, 1996, **115B**, 247–254.
48 M. Lopez, B. Paul, A. Hofmann, J. Morizzi, Q. K. Wu, S. A. Charman, A. Innocenti, D. Vullo, C. T. Supuran and S. A. Poulsen, *J. Med. Chem.*, 2009, **52**, 6421–6432.
49 R. M. Vitale, C. Pedone, P. Amodeo, J. Antel, M. Wurl, A. Scozzafava, C. T. Supuran and G. De Simone, *Bioorg. Med. Chem.*, 2007, **15**, 4152–4158.
50 C. Temperini, A. Innocenti, A. Guerri, A. Scozzafava, S. Rusconi and C. T. Supuran, *Bioorg. Med. Chem. Lett.*, 2007, **17**, 2210–2215.
51 C. Temperini, A. Scozzafava and C. T. Supuran, *Bioorg. Med. Chem. Lett.*, 2006, **16**, 5152–5156.
52 K. M. Jude, A. L. Banerjee, M. K. Haldar, S. Manokaran, B. Roy, S. Mallik, D. K. Srivastava and D. W. Christianson, *J. Am. Chem. Soc.*, 2006, **128**, 3011–3018.
53 D. K. Srivastava, K. M. Jude, A. L. Banerjee, M. Haldar, S. Manokaran, J. Kooren, S. Mallik and D. W. Christianson, *J. Am. Chem. Soc.*, 2007, **129**, 5528–5537.
54 S. Chakravarty and K. K. Kannan, *J. Mol. Biol.*, 1994, **243**, 298–309.
55 K. K. Kannan, in *Biomolecular Structure, Conformation, Function and Evolution vol 1*, Ed. R. Srinivasan, Pergamon, Oxford, 1981, pp. 165-181.
56 V. Kumar, K. K. Kannan and P. Sathyamurthi, *Acta Crystallogr., Sect. D: Biol. Crystallogr.*, 1994, **50**, 731–738.
57 V. Kumar and K. K. Kannan, *J. Mol. Biol.*, 1994, **241**, 226–232.
58 Z. Weiwei and R. Hu, *Biochem. Biophys. Res. Commun.*, 2009, **390**, 368–371.
59 E. P. Feener, *Nat. Med.*, 2007, **13**, 181–188.
60 Z. Otwinowski and W. Minor, *Methods Enzymol.*, 1997, **276**, 307–326.
61 J. Navaza, *Acta Crystallogr., Sect. A: Found. Crystallogr.*, 1994, **50**, 157–163.
62 A. T. Brünger, P. D. Adams, G. M. Clore, W. L. De Lano, P. Gros, R. W. Grosse-Kunstleve, J. S. Jiang, J. Kuszewski, M. Nilges, N. S. Pannu, R. J. Read, L. M. Rice, T. Simonson and G. L. Warren, *Acta Crystallogr., Sect. D: Biol. Crystallogr.*, 1998, **54**, 905–921.
63 T. A. Jones, J. Y. Zou, S. W. Cowan and M. Kjeldgaard, *Acta Crystallogr., Sect. A: Found. Crystallogr.*, 1991, **47**, 110–119.
64 R. A. Laskowski, M. W. MacArthur, D. S. Moss and J. M. Thornton, *J. Appl. Crystallogr.*, 1993, **26**, 283–291.